MOLECULAR AND CELLULAR BIOLOGY, Oct. 1997, p. 5707–5718 Vol. 17, No. 10
0270-7306/97/$04.00+0

Self-Association of the Single-KH-Domain Family Members Sam68, GRP33, GLD-1, and Qk1: Role of the KH Domain

TAIPING CHEN,[1] BASSAM B. DAMAJ,[1]† CONSTANCE HERRERA,[1] PAUL LASKO,[2] AND STÉPHANE RICHARD[1]*

Terry Fox Molecular Oncology Group, Lady Davis Institute for Medical Research, Sir Mortimer B. Davis Jewish General Hospital, and Departments of Oncology, Medicine, and Microbiology and Immunology, McGill University, Montreal, Quebec H3T 1E2,[1] and Department of Biology, McGill University, Montreal, Quebec H3A 1B1,[2] Canada

Received 14 March 1997/Returned for modification 23 May 1997/Accepted 23 July 1997

Sam68 is a member of a growing family of proteins that contain a single KH domain embedded in a larger conserved domain of ~170 amino acids. Loops 1 and 4 of this KH domain family are longer than the corresponding loops in other KH domains and contain conserved residues. KH domains are protein motifs that are involved in RNA binding and are often present in multiple copies. Here we demonstrate by coimmunoprecipitation studies that Sam68 self-associated and that cellular RNA was required for the association. Deletion studies demonstrated that the Sam68 KH domain loops 1 and 4 were required for self-association. The Sam68 interaction was also observed in *Saccharomyces cerevisiae* by the two-hybrid system. In situ chemical cross-linking studies in mammalian cells demonstrated that Sam68 oligomerized in vivo. These Sam68 complexes bound homopolymeric RNA and the SH3 domains of p59^{fyn} and phospholipase Cγ1 in vitro, demonstrating that Sam68 associates with RNA and signaling molecules as a multimer. The formation of the Sam68 complex was inhibited by p59^{fyn}, suggesting that tyrosine phosphorylation regulates Sam68 oligomerization. Other Sam68 family members including *Artemia salina* GRP33, *Caenorhabditis elegans* GLD-1, and mouse Qk1 also oligomerized. In addition, Sam68, GRP33, GLD-1, and Qk1 associated with other KH domain proteins such as Bicaudal C. These observations indicate that the single KH domain found in the Sam68 family, in addition to mediating protein-RNA interactions, mediates protein-protein interactions.

The K homology (KH) domain is a small protein module consisting of 70 to 100 amino acids that was originally identified as a repeated sequence in the heterogeneous nuclear ribonucleoprotein particle (hnRNP) K (33). There are over 30 proteins that have been identified in prokaryotes and eukaryotes that contain single or multiple copies of this domain (16). The KH domain is an RNA binding motif that is thought to make direct protein-RNA contacts with a three-dimensional βααββα fold (25). The RNA binding properties of the KH domain proteins were initially demonstrated for FMR1, the gene product of the human fragile X syndrome, and hnRNP K (2, 33). It has been demonstrated that multiple KH domains are required for optimal RNA binding (32). In addition, there is evidence that KH domain proteins may function as multimers. For example, FMR1 associates with FXR family members through coiled-coil motifs and may function in translation, mRNA stability, or both (34, 46).

Mutations have been isolated in a number of genes encoding KH domain proteins in various species, making the KH domain one of the protein modules with genetic data supporting its essential physiological role. In humans, gene lesions that prevent expression of the KH protein FMR1 result in the fragile X mental retardation syndrome (28, 40), the most common form of heritable mental retardation (26). The significance of the KH domain was underscored by a point mutation altering a conserved isoleucine 304 to asparagine in the second KH domain of FMR1 (7). The point mutation alters the structure of the KH domain (25) and severely impairs RNA binding activity (32). In *Caenorhabditis elegans*, GLD-1 is a cytoplasmic protein required for germ cell differentiation (12, 13, 18). Thirty-two mutant alleles of GLD-1 can be divided into six phenotypic classes (19). Alteration of GLD-1 glycine 227 results in a recessive tumorous germ line phenotype. The structure of the vigilin KH domain predicts that this conserved glycine forms part of the RNA binding surface (25). Missense mutations were identified for GLD-1 glycine 248 or 250, and this class results in masculinization of the germ line (19). The two glycines are located at the beginning of loop 4 and are not predicted to be involved in RNA binding (25). In mice, the *quaking* viable mutation severely impairs myelination, and as a result, mice develop a rapid tremor at postnatal day 10 (31). A missense mutation in the *quaking* gene product, Qk1, is embryonic lethal (9), and alteration of Qk1 expression leads to the *quaking* viable phenotype (17). In *Drosophila melanogaster*, Bicaudal C (BicC) contains five KH domains (23). Gene lesions that truncate the BicC protein or a point mutation that replaces glycine 295 with an arginine in the third KH domain is a strong allele, leading to defects in oogenesis and anterior-posterior embryonic patterning (23).

Alignment of the KH domains (16, 25) reveals a subfamily of KH-domain-containing proteins including human and murine Sam68 (29, 45), *Artemia salina* GRP33 (6), *C. elegans* GLD-1 (19), mouse Qk1 (9), human ZFM1 (38), and predicted protein BO280.11b from *C. elegans* (44). Most recently, two additional members have been identified, including the mammalian splicing factor SF1 (1) and the *Drosophila* "held-out wings" gene product (GenBank accession no. U72331). SF1 and ZFM1 are different spliced variants derived from the same gene (1). All these proteins, except BO280.11b, contain a single KH domain embedded within a larger protein domain of ~170 residues (1, 19). This single extended KH domain is approximately 26

* Corresponding author. Mailing address: Molecular Oncology Group, Lady Davis Institute, 3755 Côte Ste-Catherine Road, Montreal, Quebec, Canada H3T 1E2. Phone: (514) 340-8260. Fax: (514) 340-7576. E-mail: mcrd@musica.mcgill.ca.

† Present address: Biology Department, Pharmacopeia Inc., Princeton, NJ 08540.

amino acids longer than most other KH domains. The extra conserved amino acids are specifically localized in loops 1 and 4; loop 1 contains an extra 6 amino acids, and loop 4 contains an additional 20 (25).

The Src-associated-in-mitosis protein of 68 kDa, Sam68, was previously called p62 (21, 45) and is the only known substrate for Src-family tyrosine kinases during mitosis (14, 37). Sam68 was identified as a binding protein for various SH3- and SH2-domain-containing signaling molecules (for a review, see reference 27). Sam68 binds Src-family tyrosine kinases, the adapter protein Grb2, and phospholipase (PL) Cγ (14, 22, 29, 37, 41, 43). Most recently, Sam68 has been shown to associate with Nck (20), the poliovirus RNA-dependent RNA polymerase 3D (24), Itk/Tsk (4), Grap (39), Cbl, and Jak3 in Hayai cells (15). These interactions support the potential role for Sam68 as an adapter molecule for tyrosine kinases (29, 36). In addition to its SH3- and SH2-domain-binding property, Sam68 is an RNA-binding protein. It has been shown to bind single-stranded RNA and single-stranded and double-stranded DNA as well as homopolymeric RNA in vitro (37, 45). The RNA binding activity of Sam68 is regulated by tyrosine phosphorylation. Phosphorylation of Sam68 by the Src-family kinase $p59^{fyn}$ abolishes homopolymeric RNA binding activity in vitro (42). Although the function of Sam68 is unknown, a splice variant of Sam68, devoid of the KH domain, has been identified and implicates the KH domain of Sam68 in cell cycle progression (3).

The presence of multiple KH domains in proteins prompted us to investigate whether the single-KH-domain family member Sam68 could oligomerize. We present evidence that Sam68 can bind signaling molecules and RNA as a multimer and that Sam68 oligomerization is regulated by the tyrosine kinase $p59^{fyn}$.

MATERIALS AND METHODS

DNA constructions. The plasmid encoding His-Sam68 was generated as follows. The *Eco*RI fragment of myc-Sam68 (previously called myc-p62 [29]; missing the N-terminal 67 amino acids) was subcloned in the *Eco*RI site of His-Bluescript KS$^+$. His-Bluescript was constructed by annealing two oligonucleotides (5′-CGC GGA TCC ACC ATG GGC AGC AGC CAT CAT CAT-3′ and 5′-GCG CTC GAG GGA ATT CCC GCT GCT GTG ATG ATG ATG ATG ATG-3′) and filling in the ends with DNA polymerase I (Klenow fragment). This DNA fragment was subcloned into the *Bam*HI and *Xho*I sites of Bluescript KS$^+$ (Stratagene). HA-Sam68 was constructed by subcloning the *Eco*RI fragment of myc-Sam68 in HA-Bluescript KS$^+$. HA-Bluescript KS$^+$ was constructed by annealing two oligonucleotides (5′-TA CCC ATG GCG TAC CCC TAC GAC GTG CCC GAC-3′ and 5′-CTG GAA TTC CAG CTG GCG TAG TCG GGC ACG TC-3′) and filling in the ends with DNA polymerase I (Klenow fragment). This DNA fragment was subcloned into the *Nco*I and *Eco*RI sites of myc-Bluescript KS$^+$ (29). Underlined nucleotides denote restriction endonuclease sites.

Sam68Δ294-405 and Sam68Δ280-339 were constructed by inverse PCR with myc-Sam68 as DNA template. The sequences of the oligonucleotides used are 5′-TCT TGG CAG CTC CTC GTC CTC TCA C-3′ and 5′-TCT TCC AAG ATT CTT ACG AAG CCT ACG-3′ (Sam68Δ294-405) and 5′-TCT TGG GTT CAG GTA CTC CGT TCA A-3′ and 5′-TCT CTG GAC GTG GTG TTG GAC CAC C-3′ (Sam68Δ280-339). Sam68:294 and Sam68:330 were constructed by using the T7 promoter primer as forward primer and 5′-TAG AAT TCA GGC AGC TCC TCG TCC TCT CAC-3′ and 5′-AGG AAT TCA TGG CAC CCC TCG AGT CAC A-3′ as reverse primers, respectively. The DNA template was myc-Sam68, and the amplified fragments were digested with *Eco*RI and subcloned in myc-Bluescript KS$^+$ (29). The DNA fragment for Sam68ΔN was amplified by PCR with 5′-GAG AAT TCG TAC CCG CCT GAA CTC A-3′ and the universal reverse primer as oligonucleotides and myc-Sam68 as a DNA template. The fragment was digested with *Eco*RI and subcloned in myc-Bluescript KS$^+$. This construct deletes the N-terminal 102 amino acids of the murine Sam68 protein. Sam68:103-269 was constructed by digesting Sam68ΔN with *Xba*I and subcloning it in the *Xba*I site of Bluescript KS$^+$. The DNA fragment for Sam68:KH was amplified by the PCR with myc-Sam68 as a DNA template and oligonucleotides 5′-TAA GAA TTC GAA GCT GAA AGA ACG CGT G-3′ and 5′-TCC CTC GAG ATA TCA TCC ATC ATA AC-3′. The DNA fragment was digested with *Eco*RI and *Xho*I and subcloned in myc-Bluescript KS$^+$.

The construct containing the entire coding region of Sam68 was generated as follows. A λ ZAP II mouse brain library (Stratagene) was screened with a ^{32}P-labeled random-primed DNA fragment encompassing nucleotides 527 to 940 of the mouse Sam68 cDNA (29). Clone B contained nucleotides 2 to 1170 of the mouse Sam68 cDNA. The coding region of this clone was amplified with a forward primer that replaces the initiator methionine with an *Eco*RI site (5′-CCC GAA TTC GAG AAG AGA CGA TCC TGC CTC GCG CC-3′) and the T7 promoter primer (located at the 3′ end of the cDNA). The amplified fragment was subcloned in myc-Bluescript KS$^+$ with *Eco*RI, and this plasmid was called myc-Bluescript-B. myc-Sam68 was digested with *Sac*II, removing the sequences between the *Sac*II site in the polylinker and the *Sac*II site located in the Sam68 cDNA at nucleotide 378. The DNA fragment obtained from the digestion of myc-Bluescript-B with *Sac*II was inserted in between the *Sac*II sites of myc-Sam68. The new plasmid was called myc-Sam68f for full length.

Sam68:I→N, Sam68:G→D, Sam68:E→G, Sam68ΔL1, Sam68ΔL4, Sam68:2G→R, and Sam68ΔKH were constructed by inverse PCR with myc-Sam68f as a DNA template. The oligonucleotides were 5′-TGT ATT TCC TTG TGG TCC AAG AAT-3′ and 5′-AAC AAA AGA CTC CAG GAA GAG ACT G-3′ (Sam68:I→N), 5′-AAG AAT CTT CCC CAC AAA ATT GAA C-3′ and 5′-GAC CCA CAA GGA AAT ACA ATC A-3′ (Sam68:G→D), 5′-TAC GGA CAG CAG CTG CAT GGC GTG AGT-3′ and 5′-GGA ATT GAG AAG ATT CAG AAG GGA G-3′ (Sam68:E→G), 5′-GAC AGG TAT CAG CAC GCG TTC-3′ and 5′-GAC CTT GTG GGG AAG ATT CTT GGA-3′ (Sam68ΔL1), 5′-CCT CAA GAC AGA GAT CTT TGC ACC AGT CTC-3′ and 5′-CCT ATG GAT CTG CAT GTC TTC ATT GAA GTC-3′ (Sam68ΔL4), 5′-CCT AGA TCA ATG AGA GAC AAA GCC AAG G-3′ and 5′-CCT CAA GAC AGA GAT CTT TGC ACC AGT CTC-3′ (Sam68:2G→R), and 5′-GAG ATG GAT CTG CAT GTC TTC ATT C-3′ and 5′-GAG CAG TTC ATG TTC TTA TGA GA-3′ (Sam68ΔKH). Underlined nucleotides denote changes introduced.

The plasmid constructs were verified by dideoxynucleotide sequencing with Sequenase (U.S. Biochemical).

Cloning of *A. salina* GRP33, *C. elegans* GLD-1, and mouse Qk1 cDNAs. Total RNA was extracted from *A. salina*, *C. elegans*, and mouse brain as previously described (30). The oligonucleotides, sense and antisense, were 5′-TAC CTC GAG AAA TGG CTG CCA AAC CCG AGC AAG-3′ and 5′-TTG CTC GAG GGC AAC TCA GTA GGG TGC TG-3′ for GRP33, 5′-CAC CTC GAG GAA TGC CGT CGT GCA CCA CTC CAA C-3′ and 5′-GTG CTC GAG TTA GAA AGA GGT GTT GTT GAC TGA AG-3′ for GLD-1, and 5′-CTG GAA TTC GGT CGG GGA AAT GGA AAC GAA GG-3′ and 5′-GCT GAA TTC TAG TCC TTC ATC CAG CAA GTC-3′ for mouse Qk1. The amplified DNA fragment for the mouse Qk1 was digested with *Eco*RI and subcloned in the *Eco*RI site of myc-Bluescript KS and HA-Bluescript KS. The amplified DNA fragments for GRP33 and GLD-1 were digested with *Xho*I and subcloned in the corresponding sites in myc-Bluescript KS and HA-Bluescript KS. The plasmid constructs were verified by dideoxynucleotide sequencing with Sequenase (U.S. Biochemical) and by the Sheldon Biotechnology Institute automated sequencing facility (McGill University). The DNA sequences of GRP33, GLD-1, and Qk1 were identical to the previously reported sequences (6, 9, 19). The GLD-1 sequence obtained did not contain the leucine-leucine-lysine sequence found in the alternatively spliced GLD-1 (19). The coding sequences amplified from Qk1-7 (17) started at methionine 287 (9).

The human FMR1-coding region was amplified with the following oligonucleotides, 5′-GAA GAA TTC GGA GCT GGT GGT GGA AGT GC-3′ and 5′-TTA GAA TTC TTA GGG TAC TCC ATT CAC-3′, with pBlueBacHis2B containing the human FMR1 cDNA as a DNA template (kindly provided by Stephen Warren [40]). The amplified fragment was digested with *Eco*RI and subcloned in the *Eco*RI sites of myc-Bluescript KS and HA-Bluescript KS.

Protein expression and protein analysis. HeLa cells were transfected with the vaccinia virus T7 expression system and lysed as previously described (29). Histidine-tagged Sam68 was affinity purified with His-Bind resin (Novagen) charged with nickel according to the manufacturer's instructions. The lysis buffer was adjusted with 1× His binding buffer: 5 mM imidazole–0.5 M NaCl–20 mM Tris-HCl (pH 7.9). Samples were analyzed on sodium dodecyl sulfate (SDS)-polyacrylamide gels and transferred to nitrocellulose membranes. Immunoblotting was performed with the following monoclonal antibodies, anti-myc 9E10 (10) and antihemagglutinin (anti-HA [BAbCO]), and the following polyclonal rabbit antibodies, anti-Sam68 (Santa Cruz Biotechnology Inc.), anti-fyn (kindly provided by André Veillette), and anti-BicC antibodies. The designated primary antibody was followed by goat anti-rabbit or goat anti-mouse antibody conjugated to horseradish peroxidase (Organon Teknika-Cappel), and chemiluminescence was used for protein detection (Dupont).

The yeast two-hybrid system. The yeast two-hybrid system was obtained from Stephen Elledge (8). pAS1/Sam68 and pAS1/Sam68ΔN were constructed by amplifying the Sam68 sequences from plasmids myc-Sam68ΔN and myc-Sam68 with the T7 promoter primer and the universal reverse primer containing a *Sal*I site (5′-ACC GGT CGA CGG AAA CAG CTA TGA CCA TGA TTA C-3′). The DNA fragments were digested with *Nco*I (located at the beginning of the myc tag in myc-Bluescript KS$^+$) and *Sal*I and subcloned in similar sites in the polylinker of pAS1 (8). pACT/Sam68 has been previously described (29).

Saccharomyces cerevisiae Y190 was transformed with pACT/Sam68, pACT/Sam68 and pAS1/Sam68ΔN, pACT/Sam68 and pAS1/Sam68, pAS1/Sam68ΔN, or pAS1/Sam68. The expression of pAS1/Sam68 and pAS1/Sam68ΔN fusion proteins was verified by immunoblotting with anti-HA antibodies. The ability of

pACT/Sam68 to interact with pAS/SNF1 or pAS/lamin was determined by mating as described previously (29). The ability of the yeast to activate the *GAL1-lacZ* reporter gene was assessed by the colony lift assay and scored as white (negative) or blue (positive). The strength of the interactions was quantitated by the *O*-nitrophenyl-β-D-galactopyranoside spectrophotometric assay, and the β-galactosidase activity was expressed as units of enzyme (11).

In vitro self-association assay with His-Sam68. HeLa cells transfected with His-Sam68 and the indicated myc-Sam68 construct were lysed separately. The nuclei were removed by centrifugation, and the supernatants were mixed for 1 h on ice in the presence of 2-mg/ml heparin. The mixture was divided into two and immunoprecipitated with immunoglobulin G (IgG) (control [Sigma]) or anti-myc antibodies. The bound proteins were separated on SDS–9% polyacrylamide gels, and the proteins were transferred to nitrocellulose membranes and immunoblotted with anti-Sam68 antibodies.

RNase treatments and RNA binding analysis. RNase treatment was performed at either 4 or 37°C for 1 h with a final concentration of 1 mg of RNase A (Boehringer Mannheim) per ml. Incubating the cell lysates at 37°C without RNase was considered a mock treatment. For experiments with RNase inhibitor, RNAguard (Pharmacia) was added at a final concentration of 1,700 U/ml. Poly(U) binding was performed with poly(U)-Sepharose beads (Pharmacia) or Sepharose beads (Sigma) in lysis buffer supplemented with 2-mg/ml heparin (Sigma) for 1 h at 4°C. The beads were washed and analyzed as previously described (42). Poly(A), poly(G), and poly(C) were coupled to cyanogen-activated Sepharose beads (Sigma) at 5 mg/ml. ^{32}P-labeled cellular RNA was prepared by incubating 10^7 HeLa cells with 250-μCi/ml orthophosphate overnight. RNA was isolated with the RNeasy minikit (Qiagen) and verified on agarose gels. The labeled RNA (3×10^6 cpm) was incubated with control or anti-myc immunoprecipitates of either untransfected or transfected cells for 30 min at 4°C, washed three times, and counted. The counted samples were resuspended in sample buffer and separated by SDS-polyacrylamide gel electrophoresis (PAGE); the proteins were transferred to nitrocellulose and analyzed by immunoblotting with anti-myc antibodies.

In situ chemical cross-linking. HeLa or NIH 3T3 cells (10^7) were concentrated into 0.5 ml of phosphate-buffered saline (PBS), pH 8.0, by centrifugation and incubated at room temperature for 30 min with or without 1 mM bis(maleimido)hexane (BMH) (Sigma and Pierce) or disuccinimidyl suberate (DSS) (Pierce) as described elsewhere (35). The cells remained intact during the BMH or DSS treatments, as visualized by light microscopy and trypan blue exclusion. The cells were pelleted by centrifugation, resuspended in 75 μl of 2× sample buffer (60 mM Tris-HCl [pH 8.0], 2% SDS, 2% dithiothreitol, 10% glycerol, 0.01% bromophenol blue, 0.25 mM phenylmethanesulfonyl fluoride, and 2 mM sodium vanadate), and loaded on SDS–6.5% polyacrylamide gels. The proteins were transferred to nitrocellulose membranes and immunoblotted with anti-Sam68 polyclonal antibodies.

The poly(U) and SH3-domain binding ability of the Sam68 complex was examined by leaving HeLa cells untreated or treated with BMH in situ; the cells were lysed and incubated with poly(U)-Sepharose or affinity matrices coupled to glutathione *S*-transferase (GST)–SH3 domains as described elsewhere (29). The bound proteins were analyzed on SDS–6.5% polyacrylamide gels, transferred to nitrocellulose, and immunoblotted with anti-Sam68 antibodies.

For transfected HeLa cells, 0.5×10^7 adherent cells were incubated at room temperature for 30 min with or without 1 mM BMH. The cells were washed with PBS and either lysed in sample buffer as described above or lysed in lysis buffer and incubated with poly(U)-Sepharose or uncharged or nickel-charged His-Bind resin. The beads were washed, and the bound proteins were separated by SDS-PAGE, transferred to nitrocellulose membranes, and immunoblotted with the indicated antibody.

Characterization of the Sam68 complex. HeLa cells transfected with His-Sam68, myc-Sam68, and HA-Sam68 were left untreated or treated with BMH. The cells were lysed in lysis buffer supplemented with 50 mM Tris-HCl (pH 8.0), and the lysates were incubated with charged or uncharged His-Bind resin. The beads were washed, and the bound proteins were eluted with imidazole. The eluted proteins were dialyzed overnight with PBS to remove the excess imidazole. The buffer of the eluted protein was adjusted to 1% Triton X-100 and immunoprecipitated with anti-myc or control antibodies. The bound proteins were loaded on SDS–6.5% polyacrylamide gels, transferred to nitrocellulose membranes, and immunoblotted with anti-HA antibodies.

RESULTS

Interaction of Sam68 with itself by coimmunoprecipitation studies. To determine if Sam68 could oligomerize, we performed coimmunoprecipitation studies with HeLa cells transfected with truncated versions of epitope-tagged Sam68. Two plasmids that encoded Sam68 proteins that were shorter than the endogenous Sam68 were constructed (Fig. 1A). The histidine-tagged Sam68 (His-Sam68) contained a deletion of the N-terminal 67 amino acids and migrated with an apparent molecular mass of 60 kDa on an SDS-polyacrylamide gel. The

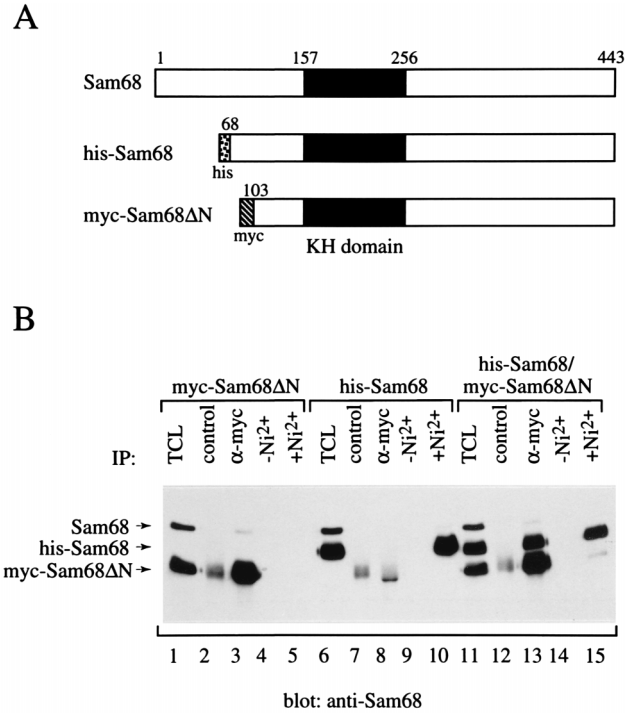

FIG. 1. Self-association of Sam68 by coimmunoprecipitation studies. (A) Schematic diagram of the truncated epitope-tagged Sam68 proteins used. The black box represents the Sam68 KH domain. The N-terminal 67 amino acids of Sam68 were replaced by six histidine residues (His tag; small box with black dots) in His-Sam68. The construct myc-Sam68ΔN is missing the N-terminal 102 amino acids of Sam68 and has a myc epitope tag (hatched box). (B) HeLa cells were transfected with the plasmids encoding myc-Sam68ΔN (lanes 1 to 5), His-Sam68 (lanes 6 to 10), or myc-Sam68ΔN plus His-Sam68 (lanes 11 to 15). The cells were lysed and immunoprecipitated (IP) with a control or anti-myc antibody or incubated with His-Bind resin uncharged ($-Ni^{2+}$) or charged with nickel ($+Ni^{2+}$). The bound proteins as well as total cell lysates (TCL) were separated on SDS–9% polyacrylamide gels, transferred to nitrocellulose, and immunoblotted with anti-Sam68 antibodies. The positions of the endogenous Sam68 (Sam68), His-Sam68, and myc-Sam68ΔN are indicated by arrows, and their approximate molecular masses are 68, 60, and 50 kDa, respectively. The broad bands observed at 50 kDa in lanes 2, 7, 8, and 12 represent the antibody heavy chains.

myc-tagged Sam68ΔN (myc-Sam68ΔN) construct contained a deletion of the N-terminal 102 amino acids and had an apparent molecular mass of 50 kDa. HeLa cells were transfected with plasmids encoding myc-Sam68ΔN, His-Sam68, or both myc-Sam68ΔN and His-Sam68 as indicated (Fig. 1B). An aliquot of the cell lysate was kept to represent total cell lysate, and the remainder was divided equally and immunoprecipitated with IgG (control) or anti-myc antibodies or incubated with uncharged or charged nickel resin. The bound proteins were separated by SDS-PAGE, transferred to nitrocellulose, and immunoblotted with anti-Sam68 antibodies. Anti-myc immunoprecipitates of cells transfected with myc-Sam68ΔN contained endogenous Sam68 (Fig. 1B, lanes 3 and 13). His-Sam68 was also observed in anti-myc immunoprecipitates, when it was cotransfected with myc-Sam68ΔN (lane 13). The nickel-charged resin was less effective in coprecipitating Sam68. Nevertheless, endogenous Sam68 (lane 10) and myc-Sam68ΔN (lane 15) coprecipitated with His-Sam68. These observations demonstrated that Sam68 self-associated and that the N-terminal 102 amino acids were not required for self-association.

Self-association of Sam68 by the yeast two-hybrid system. The yeast two-hybrid system was used to investigate whether the interaction between Sam68 could occur in yeast cells.

TABLE 1. Detection of self-association of Sam68 by using the yeast two-hybrid system[a]

DNA-binding hybrid	Activation hybrid	Colony color	β-Gal activity	*n*
Sam68	Sam68	Blue	7.28 ± 2.43	18
Sam68ΔN	Sam68	Blue	15.36 ± 8.54	6
Sam68	None	White	0.087 ± 0.076	4
Sam68ΔN	None	White	0.837 ± 0.23	4
None	Sam68	White	0.31 ± 0.087	6
SNF1	Sam68	White	ND	3
Lamin	Sam68	White	ND	3

[a] The yeast strain Y190 was transformed with plasmids containing Sam68 and Sam68ΔN in pACT (activation hybrid) or pAS (DNA-binding hybrid) as indicated. The strength of the interactions was quantitated by the *O*-nitrophenyl-β-D-galactopyranoside spectrophotometric assay, and the activity of β-galactosidase is expressed as units of enzyme (Miller units). ND, not determined.

GAL4 DNA binding hybrids that contained Sam68 or Sam68ΔN in the plasmid pAS-1 were constructed (8). The yeast strain Y190 was transformed with each of these plasmids alone or in combination with a plasmid expressing Sam68 as a GAL4-transactivating hybrid (8). Yeast cells were plated on appropriate selective media and assayed for β-galactosidase activity. The *lacZ* gene was activated, and the colonies turned blue only in the yeast expressing Sam68-Sam68 and Sam68ΔN-Sam68 in both hybrids (Table 1). The interaction was strong, with β-galactosidase activities greater than 7 Miller units compared to those of the controls, which did not exceed 1 (Table 1). The Sam68-Sam68 interaction was specific because no interaction between Sam68 and SNF1 or lamin was observed as described previously (Table 1) (29).

In situ chemical cross-linking of Sam68. In situ chemical cross-linking studies with human and mouse cells were performed to determine whether Sam68 formed dimers, trimers, or larger complexes. HeLa cells were treated or not with BMH and lysed in sample buffer, and the complexes were separated by SDS-PAGE and immunoblotted with anti-Sam68 antibodies. In addition to the 68-kDa band representing monomeric Sam68, a band with an apparent molecular mass of 200 kDa was observed (Fig. 2A, lane 2). To confirm that this was not an artifact of the BMH cross-linker, we treated cells in situ with another chemical cross-linker. A similar Sam68 complex was also observed with DSS cross-linking (Fig. 2A, lane 4). The complex could be observed also in mouse cells, as BMH treatment of NIH 3T3 cells resulted in a similar Sam68 complex (Fig. 2B).

Oligomerization of Sam68 in vivo. As the apparent molecular mass of the Sam68 complex was similar to the mass predicted for a Sam68 trimer, we investigated whether two and three molecules of Sam68 were present in the complex. HeLa cells were transfected with two different epitope-tagged Sam68 molecules, His-Sam68 and myc-Sam68. The cells were mock or BMH treated, lysed, and incubated with uncharged or charged nickel beads to purify the histidine-tagged Sam68. The bound proteins were separated by SDS-PAGE, transferred to nitrocellulose, and immunoblotted with anti-myc antibodies. A band corresponding to the Sam68 complex was detected (Fig. 2C, lane 4). This demonstrated that at least two Sam68 molecules were present in the complex. To verify that a third Sam68 molecule was present in the complex, HeLa cells were transfected with three different epitope-tagged Sam68 molecules. The cells were mock (lanes 1 to 4) or BMH (lanes 5 to 8) treated, lysed, and incubated with uncharged or charged nickel beads to purify the histidine-tagged Sam68 ("1st IP" in Fig. 2D). The bound proteins were eluted from the beads and reimmunoprecipitated for myc-Sam68 with control or anti-myc antibodies ("2nd IP" in Fig. 2D). The bound complexes were separated by SDS-PAGE, transferred to nitrocellulose membranes, and immunoblotted with anti-HA antibodies to detect

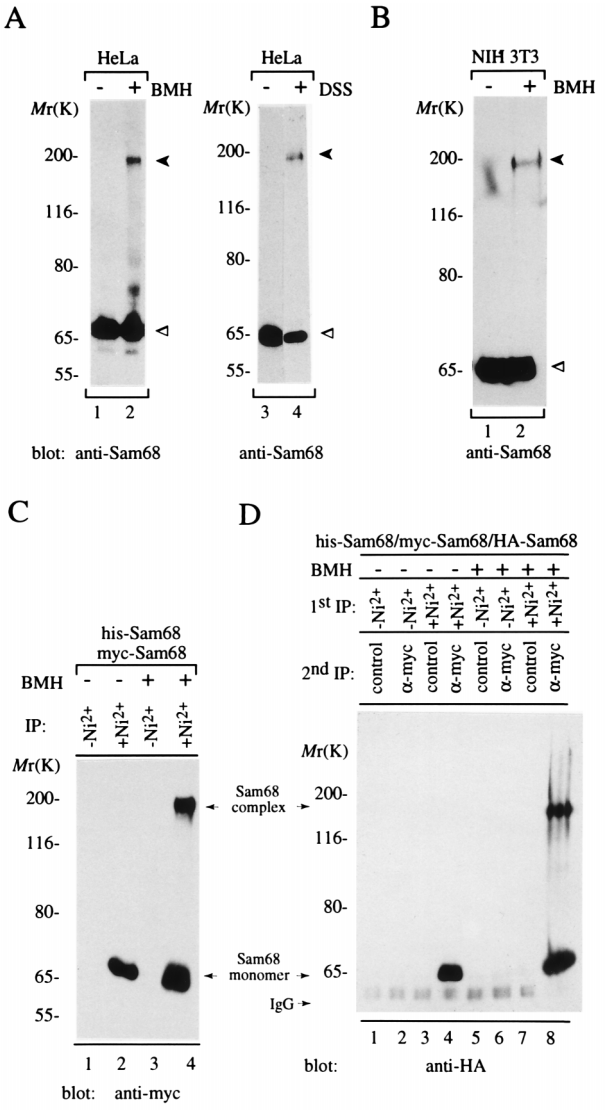

FIG. 2. In situ chemical cross-linking of Sam68. (A) HeLa cells were mock treated (lanes 1 and 3), BMH treated (lane 2), or DSS treated (lane 4) in situ. The cells were lysed in sample buffer and separated by SDS-PAGE. The content was transferred to a nitrocellulose membrane and immunoblotted with anti-Sam68 antibodies. (B) NIH 3T3 cells were mock or BMH treated and analyzed as for panel A. The open arrowhead represents the un-cross-linked Sam68, and the solid arrowhead represents the cross-linked Sam68 complex. (C) The plasmids encoding His-tagged and myc-tagged Sam68 were transfected in HeLa cells. The cells were left untreated or treated with BMH in situ. The cells were lysed, and the lysates were incubated with His-Bind resin in the presence or absence of nickel. The bound proteins were eluted from the beads and separated on SDS–6.5% polyacrylamide gels, transferred to nitrocellulose, and immunoblotted with anti-myc antibodies. (D) The plasmids encoding His-tagged, myc-tagged, and HA-tagged Sam68 were transfected in HeLa cells. The cells were left untreated or treated with BMH in situ. The cells were lysed, and the lysates were incubated with His-Bind resin in the presence or absence of nickel (first immunoprecipitation [1st IP]). The bound proteins were eluted from the beads and reimmunoprecipitated with control or anti-myc antibodies (second immunoprecipitation [2nd IP]). The proteins were separated on SDS–6.5% polyacrylamide gels, transferred to nitrocellulose, and immunoblotted with anti-HA antibodies. The relative molecular weight markers are shown on the left of each panel in thousands. IP, immunoprecipitation.

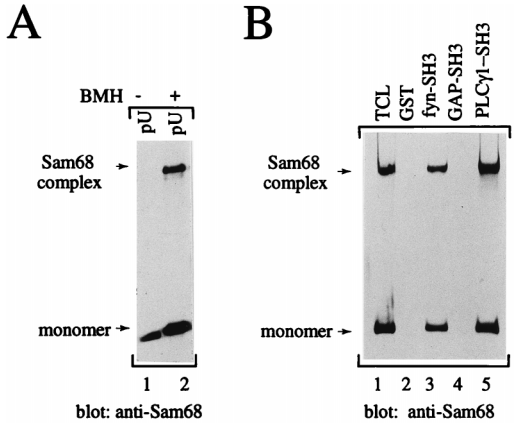

FIG. 3. (A) The Sam68 complex binds RNA. HeLa cells were left untreated (lane 1) or BMH treated in situ (lane 2), lysed, and incubated with poly(U)-Sepharose. The bound proteins were analyzed on SDS–6.5% polyacrylamide gels, transferred to nitrocellulose membranes, and immunoblotted with anti-Sam68 antibodies. (B) The Sam68 complex associates with the SH3 domains of $p59^{fyn}$ and PLCγ1. HeLa cells were BMH treated in situ, lysed, and incubated with affinity matrices containing GST, GST-fynSH3, GST-GAP-SH3, and GST-PLCγ1-SH3. The bound proteins were analyzed as for panel A. The Sam68 complex and the Sam68 monomer are indicated. TCL, total cell lysates.

HA-Sam68. A band with an approximate molecular mass of 190 kDa was observed (Fig. 2D, lane 8). These findings demonstrated that at least three different Sam68 molecules were associated with each other, suggesting that Sam68 forms homotrimers. However, it is possible that three Sam68 molecules associated as a result of an interaction between two separate complexes; therefore, the cross-linked Sam68 complex could also consist of a Sam68 dimer that migrates with an aberrant molecular mass of 190 kDa, or the complex could consist of a Sam68 dimer with an unknown protein with an apparent molecular mass of 60 to 70 kDa that is not $p59^{fyn}$ (see below). Although these experiments do not address which of the possibilities is occurring, they clearly show that Sam68 oligomerizes in vivo. The complex in Fig. 2C and D had a faster mobility compared to that in Fig. 2A and B because the epitope-tagged Sam68 molecules migrate between 60 and 65 kDa due to the absence of the N-terminal 67 amino acids. The 65-kDa band observed in lane 4 (Fig. 2D) indicated that the Sam68 complex was purified, but since the complex was not treated with BMH, the complex was dissociated in the sample buffer, and monomeric HA-Sam68 was detected.

The cross-linked Sam68 complex associates with SH3 domains and homopolymeric RNA. We examined whether the Sam68 complex formed after in situ chemical cross-linking could associate with homopolymeric RNA in vitro. HeLa cells were left untreated or treated in situ with BMH, lysed, and examined for their ability to associate with poly(U)-Sepharose. The 200-kDa Sam68 complex observed with BMH treatment associated with poly(U)-Sepharose (Fig. 3A, lane 2). These findings demonstrated that Sam68 can associate with RNA as a multimer. As Sam68 is known to associate with the SH3 domains of $p59^{fyn}$ and PLCγ1 (29), we examined whether Sam68 could associate with these domains as a multimer. Indeed, this was the case, as the cross-linked Sam68 complex associated with the SH3 domain of $p59^{fyn}$ and PLCγ1 but not p120rasGAP (Fig. 3B). This binding specificity was similar to what has been described previously (29). Sam68, therefore, has the capability to associate with both SH3-domain-containing proteins and RNA as a multimer.

Mapping the Sam68 homopolymeric RNA binding domain. We next wanted to map the homopolymeric RNA binding domain of Sam68 and determine whether it overlapped with the region required for self-association. Sam68 contains two putative RNA binding domains: the N-terminal RGG box, which consists of a single RGG repeat, and the KH domain (5). We transfected a series of myc-tagged Sam68 constructs containing deletions or amino acid substitutions in HeLa cells and examined their ability to associate with homopolymeric RNA. Poly(U) covalently coupled beads were used because no known physiological RNA targets have been identified for Sam68 and poly(U) has been previously shown to associate with Sam68 (37). The full-length murine Sam68 protein bound poly(U)-Sepharose beads as well as Sam68 proteins containing N-terminal deletions of 67 and 102 residues (compare Sam68 with Sam68Δ1-67 and Sam68ΔN [Fig. 4A]), suggesting that the RGG box is not required. In contrast, a large deletion within the KH domain abolished the poly(U) binding activity of Sam68 (Fig. 4A, Sam68ΔKH). However, the KH domain alone was not sufficient to associate with poly(U)-Sepharose (Fig. 4A, Sam68:KH). These data demonstrate that the KH domain of Sam68 is necessary but not sufficient for the homopolymeric RNA binding activity.

Deletion of the C-terminal 113 residues had no effect on poly(U) binding activity of Sam68 (Sam68:330 [Fig. 4A]). However, deletion of the C-terminal 149 or 174 amino acids abolished poly(U) binding (Fig. 4A, Sam68:294 and Sam68:103-269). This region between residues 294 and 330 is rich in arginine-glycine (RG) repeats (45). The Sam68:294 protein contains 4 RG repeats, whereas Sam68:330 contains 11. Internal deletions removing amino acids 295 to 404 had no effect on poly(U) binding (Sam68:Δ294-405). The deletion of amino acids 281 to 338 maintained some poly(U) binding activity (Sam68:Δ280-339 [Fig. 4A]). Sam68:Δ280-339 contains one RG repeat, and Sam68:Δ294-405 contains four. We interpret these data as suggesting that approximately 100 amino acids C-terminal to the KH domain are required to stabilize poly(U) binding in the presence of heparin and that the number of RG repeats might be irrelevant.

Point mutations previously shown to have physiological effects for FMR1, GLD-1, and Qk1 were introduced in Sam68 and tested for their ability to affect homopolymeric RNA binding activity. The FMR1 mutation of isoleucine 304 to asparagine has been shown to severely reduce poly(U) binding activity (32). To investigate the role of this isoleucine in Sam68 poly(U) binding, we substituted asparagine for the equivalent isoleucine 184 in Sam68 and confirmed that it had severely impaired poly(U) binding activity (Fig. 4A, Sam68:I→N). The role of GLD-1 glycine 227 is unknown, but it has been predicted to contact RNA directly (25). The equivalent mutation in Sam68 was introduced and severely impaired poly(U) binding activity, confirming its role in RNA binding (Sam68: G→D). Three other mutations were observed in the KH domain of GLD-1, a proline (217)-to-leucine change in loop 1 and a glycine (248 or 250)-to-arginine change in loop 4 (19). To investigate the roles of loops 1 and 4 in poly(U) binding, we shortened each loop separately to the size of the corresponding loop present in the first KH domain of FMR1 (40). The deletion of Sam68 loop 1 had little or no effect on poly(U) binding activity (Fig. 4A, Sam68:ΔL1). In contrast, deletion of loop 4 had reduced poly(U) binding activity (Sam68:ΔL4). The replacement of glycines 199 and 201 with arginines also resulted in reduced poly(U) binding activity, similar to that observed with Sam68:ΔL4 (Fig. 4A, Sam68:2G→R). The point mutation identified in the mouse *quaking* gene (9) was also introduced in Sam68, replacing glutamic acid 128 with a glycine. This muta-

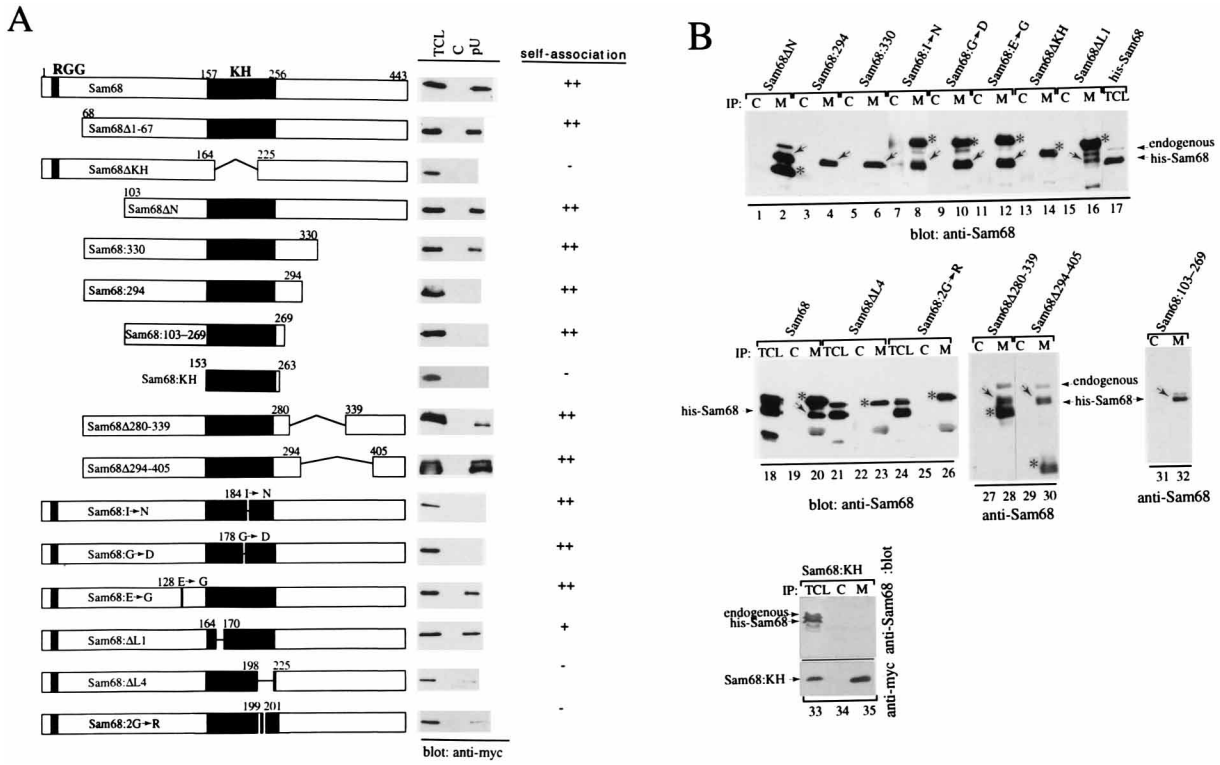

FIG. 4. Mapping the poly(U) binding and self-association domains. (A) A schematic diagram representing the various myc-Sam68 constructs is shown on the left. The large black boxes represent the KH domain, and the small black boxes represent the arginine-glycine-glycine sequence (RGG). Δ indicates a deletion, and → represents an amino acid substitution. The thin line denotes the absence of amino acid sequences or amino acid substitutions. Each plasmid construct was transfected in HeLa cells, the cells were lysed, and the cell lysates containing 2-mg/ml heparin were incubated with Sepharose (control [C]) or poly(U)-Sepharose (pU). The bound proteins were separated by SDS-PAGE, transferred, and immunoblotted with anti-myc antibodies (shown on the right). The self-association data shown in panel B are summarized: ++, +, and − denote strong, moderate, and no self-association, respectively. (B) HeLa cell lysates containing His-Sam68 were mixed with HeLa cell lysates containing the indicated Myc-tagged protein. The mixed lysates were divided equally and immunoprecipitated (IP) with control (C) or anti-myc (M) antibodies. The presence of His-Sam68 in myc immunoprecipitations was analyzed by SDS-PAGE, transferred to nitrocellulose, and immunoblotted with anti-Sam68 antibodies. The endogenous Sam68 and His-Sam68 are indicated. Lane 17 represents the input His-Sam68 for lanes 1 to 16. Lanes 18, 21, 24, and 33 represent the input after mixing. The arrows represent His-Sam68, and the asterisks represent myc-Sam68 constructs. In lanes 4, 6, and 32, myc-Sam68 constructs were expressed to levels seen in panel A (data not shown). The slower-migrating band in lane 2 is endogenous Sam68. Longer exposure of lanes 4, 6, and 32 reveals endogenous Sam68 (data not shown). The myc expression of Sam68:KH is shown in the lower panel for lanes 33 to 35. The upper panel for lanes 33 to 35 was immunoblotted with anti-Sam68 antibodies. TCL, total cell lysates.

tion had no effect on poly(U) binding activity (Fig. 4A, Sam68: E→G).

Localization of the Sam68 self-association region. The region responsible for Sam68 self-association was delineated by examining the ability of various myc-Sam68 proteins to associate with His-Sam68. Since the molecular mass of several myc-Sam68 constructs was approximately 68 kDa, we examined the ability of the myc-Sam68 proteins to associate with a shorter Sam68 protein truncated in the N-terminal 67 amino acids (His-Sam68). The ability to associate with His-Sam68 correlated with the ability to associate with endogenous Sam68 and to form cross-linked Sam68 complexes in vitro (Fig. 1 and data not shown). HeLa cells were transfected with various myc-Sam68 constructs and mixed with HeLa lysates containing His-Sam68. The lysates were immunoprecipitated with control or anti-myc antibodies. The bound proteins were separated by SDS-PAGE, transferred to nitrocellulose membranes, and immunoblotted with anti-Sam68 antibodies. myc immunoprecipitates of Sam68ΔN, Sam68:294, Sam68:330, Sam68:I→N, Sam68G→D, Sam68:E→G, Sam68, Sam68Δ280-339, Sam68Δ294-405, and Sam68:103-269 contained abundant levels of His-Sam68 (Fig. 4B, lanes 2, 4, 6, 8, 10, 12, 20, 28, 30, and 32, respectively). In contrast, myc immunoprecipitates of Sam68ΔKH, Sam68ΔL4, Sam68:2G→R, and Sam68:KH did not coprecipitate any detectable levels of His-Sam68 (lanes 14, 23, 26, and 35, respectively). Sam68ΔL1 constantly coprecipitated reduced levels of His-Sam68 (lane 16). The equivalent GLD-1 glycine 227 (Sam68:G→D) and the FMR1 isoleucine 304 (Sam68:I→N) in Sam68, essential for poly(U) binding, were not required for self-association. The *quaking* missense mutation when introduced in Sam68 had no effect on the ability of Sam68 to self-associate or to bind homopolymeric RNA. We determined that the minimal region required for Sam68 self-association was from residues 103 to 269. Within this region, the KH domain loops 1 and 4 were essential. The fact that the KH domain alone (Sam68:KH) did not associate with His-Sam68 suggests that the 50 residues N-terminal to the KH domain are required and might be important to maintain the structure of the KH domain for self-association.

Investigation of the role of RNA in self-association of Sam68. To further examine the role of RNA in Sam68 self-association, cell lysates were treated with RNase before and after mixing. HeLa cell lysates expressing His-Sam68 or myc-Sam68ΔN were lysed separately, and the cell lysates were treated with or without RNase separately and then mixed (Fig. 5A, lanes 1 to 6) or mixed and then treated with or without RNase (premix; lanes 7 to 12). An aliquot of the mixed proteins was kept to represent total cell lysate and to demonstrate

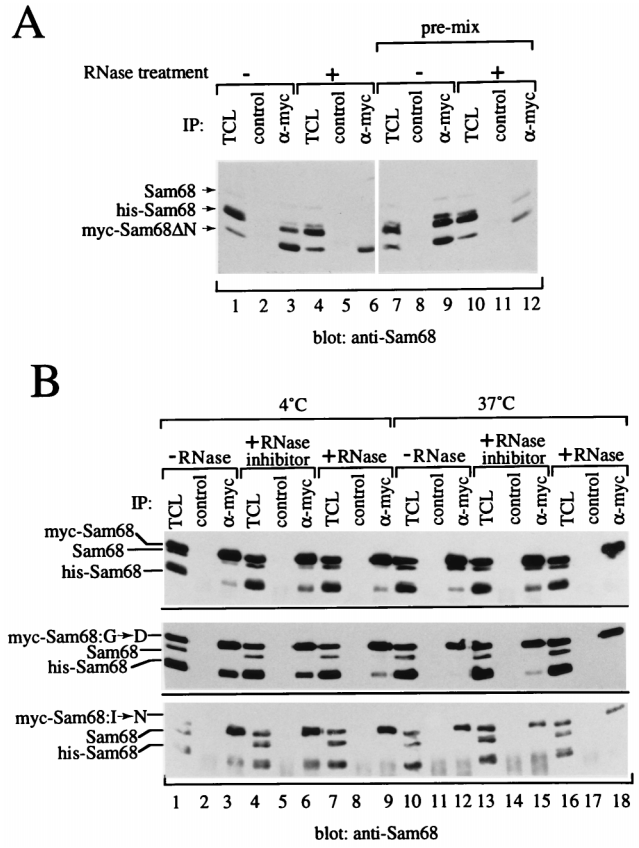

FIG. 5. The role of RNA in mediating Sam68 self-association. (A) HeLa cells were transfected with His-Sam68 or myc-Sam68ΔN and lysed separately. Cell lysates were mock treated (lanes 1 to 3) or treated with RNase at 37°C before mixing (lanes 4 to 6). In lanes 7 to 12, cell lysates were mock treated and RNase treated at 37°C after mixing. After the RNase treatment and the mixing, cell lysates were immunoprecipitated (IP) with control (lanes 2, 5, 8, and 11) or anti-myc (lanes 3, 6, 9, and 12) antibodies. The bound proteins as well as total cell lysates (TCL) were separated on SDS–9% polyacrylamide gels, transferred, and immunoblotted with anti-Sam68 antibodies. The positions of endogenous Sam68 (Sam68), His-Sam68, and myc-Sam68ΔN are indicated on the left. (B) HeLa cells were transfected with myc-Sam68, myc-Sam68:G→D, myc-Sam68:I→N, and His-Sam68 separately. Each lysate was incubated at 4 or 37°C for 1 h in the absence of RNase (−RNase), in the presence of RNase inhibitor (+RNase inhibitor), or in the presence of RNase (+RNase). The myc-expressing lysates were mixed with His-Sam68 at 4°C for 1 h and immunoprecipitated (IP) with IgG (control) or anti-myc antibodies. The bound proteins were separated on SDS–9% polyacrylamide gels and immunoblotted with anti-Sam68 antibodies. The migration of the Sam68 constructs is shown on the left. Each experiment shown is a representation of at least three separate experiments. In the lowest panel (myc-Sam68:I→N), the diffuse bands seen in lanes 5, 8, 9, 11, 12, 14, 15, 17, and 18 represent the heavy chain of the antibodies. TCL, total cell lysates.

that Sam68 did not degrade during the RNase treatment. The His-Sam68–myc-Sam68ΔN mixture was immunoprecipitated with IgG (control) or anti-myc antibodies. myc immunoprecipitates contained abundant levels of His-Sam68 and endogenous Sam68 in the mock-treated samples (Fig. 5A, lanes 3 and 9). RNase treatment of the His-Sam68- and myc-Sam68ΔN-containing HeLa cell lysates prior to mixing resulted in little if any His-Sam68 in myc immunoprecipitates (lane 6). If the myc-Sam68ΔN and His-Sam68 lysates were mixed before RNase treatment, His-Sam68 was detected in myc immunoprecipitates, albeit at a lower level than without RNase treatment (compare lanes 9 and 12). These data strongly imply that cellular RNA is required for the initial steps of the complex formation. Once the complex is formed, RNase treatment has no effect because either the complex is protecting a fragment of RNA required to stabilize the complex or RNA is no longer required once the complex is formed. The weak association observed after mixing and after RNase treatment (Fig. 5A, lane 12) suggests that RNA is required to stabilize the complex.

Although the RNase treatment experiments demonstrated that cellular RNA was required for Sam68 self-association, several Sam68 proteins that self-associated did not bind homopolymeric RNA (Fig. 4, Sam68:294, Sam68:103-269, Sam68:I→N, and Sam68:G→D). To address this issue, similar mixing-RNase treatment experiments with the full-length Sam68 as well as two homopolymeric RNA-defective proteins, Sam68:I→N and Sam68:G→D, were performed. The lysates for myc-Sam68, myc-Sam68:I→N, Sam68:G→D, and His-Sam68 were incubated without RNase, with an RNase inhibitor, or with RNase at 4 or 37°C for 1 h; mixed; and immunoprecipitated with control or anti-myc antibodies. The bound proteins were separated by SDS-PAGE and analyzed by immunoblotting with anti-Sam68 antibodies. myc-Sam68 associated with both endogenous Sam68 and His-Sam68 in the absence of RNase treatment (Fig. 5B, top panel, lanes 3 and 12). The addition of an RNase inhibitor consistently increased the amount of His-Sam68 associating with myc-Sam68 (lanes 6 and 15). RNase treatment at 37°C completely abolished association between myc-Sam68 and His-Sam68 (lane 18), as was observed for myc-Sam68ΔN (Fig. 5A, lane 6). RNase treatment at 4°C had no effect on self-association of myc-Sam68 (Fig. 5B, lane 9).

His-Sam68 associated with myc-Sam68:G→D at 4°C (Fig. 5B, middle panel, lane 3) as observed previously in Fig. 4B. Treatment with the RNase inhibitor at 4°C had no effect (Fig. 5B, lane 6), and RNase treatment at 4°C slightly reduced self-association (lane 9). However, myc immunoprecipitates of myc-Sam68:G→D contained very little His-Sam68 at 37°C compared to 4°C (Fig. 5B, middle panel; compare lanes 3 and 12). To investigate whether the RNases from the cell lysates were preventing the association, we incubated the lysates with RNase inhibitors. Interestingly, this treatment consistently increased the association between Sam68:G→D and His-Sam68 (lane 15). The addition of exogenous RNase completely abrogated the association between Sam68:G→D and His-Sam68 (lane 18). We next tested whether Sam68:I→N also required RNA for self-association. myc immunoprecipitates of Sam68:I→N contained His-Sam68 at 4°C (Fig. 5B, lower panel, lane 3) as described for Fig. 4B. This association was increased with an RNase inhibitor (lane 6) and was completely abolished with RNase treatment at 4°C or any incubation at 37°C (lanes 7 to 18). Our findings suggest that Sam68:I→N and Sam68:G→D require RNA to self-associate with Sam68. The RNA bound by these proteins appears to be loosely associated or bound with low affinity because RNase treatment at 4°C or incubation at 37°C diminished or abolished the association.

Although Sam68:I→N and Sam68:G→D self-associated, they were inactive in homopolymeric RNA binding in vitro (Fig. 4A). We also wanted to confirm that the cellular RNA binding capabilities of these proteins were impaired. Sam68, Sam68:I→N, and Sam68:G→D were expressed in HeLa cells and immunoprecipitated with control or anti-myc antibodies. The immunoprecipitates were washed and incubated with labeled cellular RNA. As shown in Fig. 6A, Sam68 associated with cellular RNA as described previously (45), whereas both Sam68:I→N and Sam68:G→D proteins were unable to associate with cellular RNA. These findings demonstrate that although Sam68:I→N and Sam68:G→D associate with Sam68, the complexes are unable to bind RNA.

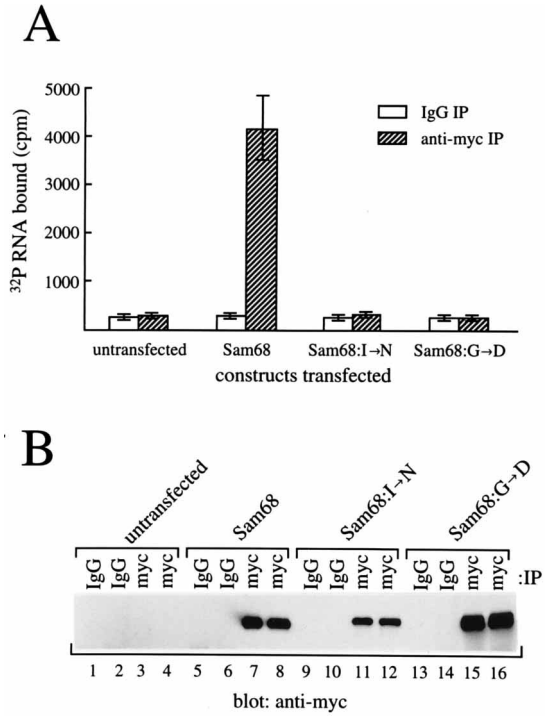

FIG. 6. The Sam68:I→N and Sam68:G→D proteins do not associate with cellular RNA. (A) HeLa cells or HeLa cells transfected with Sam68, Sam68:I→N, or Sam68:G→D were immunoprecipitated with a control IgG antibody (white bars) or anti-myc antibody (striped bars). The immunoprecipitated proteins were incubated with ^{32}P-labeled total RNA. The beads were washed, and the radioactivity associated with them was quantitated. Each bar represents the mean ± standard error of at least three separate experiments. (B) A typical representation of the expression of the myc-tagged constructs is shown. IP, immunoprecipitation.

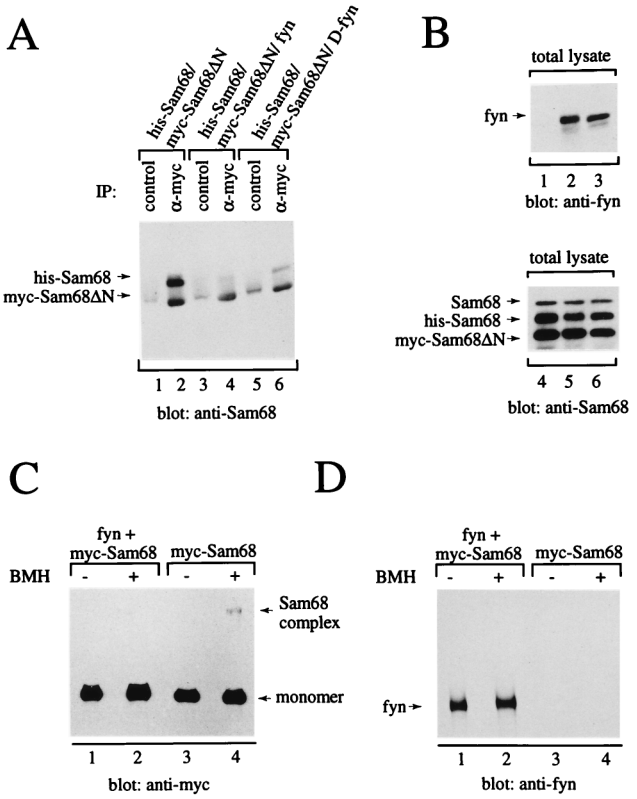

FIG. 7. Self-association of Sam68 is severely impaired by p59^{fyn}. (A) His-Sam68 was cotransfected with myc-Sam68ΔN in HeLa cells alone (lanes 1 and 2), in the presence of p59^{fyn} (lanes 3 and 4), or in the presence of kinase-inactive p59^{fyn} (dead fyn [D-fyn], lanes 5 and 6). The cells were lysed and immunoprecipitated (IP) with control or anti-myc antibodies. The bound proteins were separated by SDS-PAGE and immunoblotted with anti-Sam68 antibodies. The positions of His-Sam68 and myc-Sam68ΔN are indicated on the left. The bands with the size of myc-Sam68ΔN in lanes 1, 3, and 5 represent the antibody heavy chain. (B) Equivalent expression levels of p59^{fyn} were obtained for cells transfected with His-Sam68/myc-Sam68ΔN/fyn (lane 2) or His-Sam68/myc-Sam68ΔN/D-fyn (lane 3). Lane 1, HeLa cells transfected with His-Sam68/myc-Sam68ΔN. Equivalent expression levels of His-Sam68 and myc-SamΔN proteins were also obtained for cells transfected with His-Sam68/myc-Sam68ΔN (lane 4), His-Sam68/myc-Sam68ΔN/fyn (lane 5), or His-Sam68/myc-Sam68ΔN/D-fyn (lane 6). (C and D) Cells expressing myc-Sam68 with (lanes 1 and 2) or without (lanes 3 and 4) p59^{fyn} were left untreated (lanes 1 and 3) or treated in situ with BMH (lanes 2 and 4). The cells were lysed in sample buffer, and the proteins were separated on SDS–6.5% polyacrylamide gels, transferred to nitrocellulose membranes, and immunoblotted with anti-myc antibodies (C) or anti-p59^{fyn} antibodies (D). The positions of the un-cross-linked (monomer) or cross-linked (Sam68 complex) myc-Sam68 and p59^{fyn} are indicated by arrows.

The kinase activity of fyn abrogates self-association. The Src-family tyrosine kinase, p59^{fyn}, phosphorylates Sam68 in vivo when coexpressed in HeLa cells (29). To determine whether p59^{fyn} affected Sam68 self-association, HeLa cells were transfected with constructs encoding myc-Sam68ΔN and His-Sam68 alone, in the presence of p59^{fyn}, or in the presence of kinase-inactive p59^{fyn} (D-fyn [42]). The cells were lysed and immunoprecipitated with control or anti-myc antibodies. The bound proteins were separated by SDS-PAGE and immunoblotted with anti-Sam68 antibodies. His-Sam68 coprecipitated with myc-Sam68ΔN in the absence of fyn (Fig. 7A, lane 2). The cotransfection of p59^{fyn} significantly reduced the amount of His-Sam68 coprecipitating with myc-Sam68ΔN (lane 4), which was partially restored by D-fyn (lane 6). The expression levels of fyn and D-fyn (Fig. 7B, lanes 1 to 3) as well as of myc-Sam68ΔN and His-Sam68 (Fig. 7B, lanes 4 to 6) were equivalent. Since we have shown elsewhere that the effect of fyn compared to D-fyn was the tyrosine phosphorylation of Sam68 (42), our observations suggest that tyrosine phosphorylation regulates self-association.

The effect of fyn on in situ Sam68 complex formation was also tested. In situ cross-linking of cells expressing myc-Sam68 resulted in Sam68 complex formation (Fig. 7C, lane 4), which was severely reduced or abolished when fyn was coexpressed (Fig. 7C, lane 2). The same membrane was immunoblotted with anti-fyn antibodies (Fig. 7D). Besides the monomeric form of p59^{fyn} expressed in lanes 1 and 2, no higher-molecular-mass-containing complex was observed with BMH treatment (lane 2). These data demonstrate that p59^{fyn} is not a component of the Sam68 complex and that p59^{fyn} regulates oligomerization of Sam68 in vivo.

Characterization of GLD-1, GRP33, and Qk1 RNA and protein binding activities. The cDNAs encoding the *A. salina* GRP33, the *C. elegans* GLD-1, and the mouse Qk1 were expressed in HeLa cells as myc epitope-tagged proteins. The ability of GRP33, GLD-1, and Qk1 to bind homopolymeric RNA was compared with that of Sam68. Sam68 bound both poly(A)- and poly(U)-Sepharose (Fig. 8A, lanes 1 to 6). The poly(A) binding activity was weaker than the poly(U) binding activity, consistent with the competition data previously obtained by Taylor and Shalloway (37). GRP33 bound both poly(A)- and poly(U)-Sepharose, similar to Sam68 (Fig. 8A, lanes 13 to 18). GLD-1 bound poly(U)-Sepharose (Fig. 8A, lanes 7 to 12), and surprisingly, Qk1 did not bind any homopolymeric RNA (Fig. 8A, lanes 19 to 24). The inability of

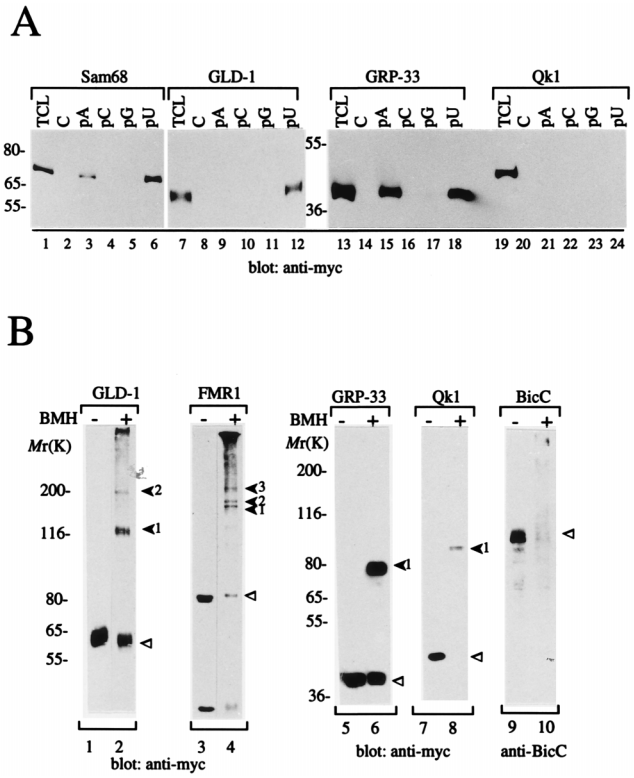

FIG. 8. RNA binding characteristics and chemical cross-linking of GRP33, GLD-1, and Qk1. (A) myc-tagged Sam68, GLD-1, GRP33, and Qk1 were expressed in HeLa cells. The cells were lysed, and an aliquot was kept for total cell lysate (TCL) or incubated with control Sepharose (C) or poly(A)-, poly(C)-, poly(G)-, or poly(U)-Sepharose beads in the presence of 2-mg/ml heparin. The bound proteins were separated by SDS-PAGE, transferred to nitrocellulose, and immunoblotted with anti-myc antibodies. The molecular mass markers are shown on the left in kilodaltons. (B) HeLa cells transfected with myc-GLD-1, myc-FMR1, myc-GRP33, myc-Qk1, and BicC were left untreated or treated in situ with BMH. The cells were lysed in sample buffer, and the proteins were separated on SDS–6.5% polyacrylamide gels, transferred to nitrocellulose membranes, and immunoblotted with anti-myc or BicC antibodies. The open arrowheads indicate the monomeric proteins, and the solid arrowheads represent the cross-linked complexes. The relative molecular weight markers are shown on the left in thousands.

Qk1 to bind homopolymeric RNA suggests that for Qk1 homopolymeric RNA may not mimic its cellular RNA targets. To verify this hypothesis and to examine whether GRP33 and GLD-1 associated with cellular RNA, ^{32}P-labeled cellular RNA from HeLa cells was incubated with anti-myc immunoprecipitates of HeLa cells expressing Qk1, GRP33, and GLD-1 (Table 2). GLD-1 bound about 0.04% of the input RNA whereas GRP and Qk1 bound 0.55 and 0.17%, respectively. The weaker RNA binding activity of GLD-1 may suggest that *C. elegans* GLD-1 has few RNA targets in HeLa cells. These findings show that GLD-1, GRP33, and Qk1 are RNA-binding proteins.

We performed in situ chemical cross-linking studies to determine whether GRP33, GLD-1, Qk1, FMR1, and BicC formed a single distinct complex as observed for Sam68. BMH addition of myc-GLD-1-transfected cells resulted in two distinct bands. The approximate molecular masses were 120 and 200 kDa, representing potential dimers and trimers (Fig. 8B, lanes 1 and 2). The three distinct bands that were observed after BMH treatment of myc-FMR1-transfected cells had approximate molecular masses ranging from 160 to 210 kDa (lanes 3 and 4). These complexes most likely represent FMR1

TABLE 2. Association of GRP33, Qk1, and GLD-1 with cellular RNA[a]

Construct transfected	IP Ab	^{32}P-RNA bound	*n*	% Bound[b]
None	IgG	259 ± 122	6	<0.01
	Anti-myc	263 ± 108	6	<0.01
myc-GRP33	IgG	235 ± 120	6	<0.01
	Anti-myc	16,362 ± 2,192	6	0.55
myc-Qk1	IgG	251 ± 114	6	<0.01
	Anti-myc	5,243 ± 847	6	0.17
myc-GLD-1	IgG	282 ± 104	6	<0.01
	Anti-myc	1,342 ± 36	6	0.04

[a] HeLa cells transfected with myc-GRP33, -GLD-1, or -Qk1 were lysed and immunoprecipitated (IP) with IgG or anti-myc antibodies (Ab). The beads were washed and incubated with ^{32}P-labeled total cellular RNA. The bound RNA was quantitated and expressed as counts per minute ± the standard errors of the means.

[b] Bound RNA as a percentage of input RNA.

homodimers and FMR-FXR heterodimers (46). BMH treatment of GRP33- or Qk1-transfected cells resulted in a single complex that potentially represents homodimers (lanes 5 to 8). The BMH pattern obtained with BicC was different and contained many distinct bands after chemical cross-linking, suggesting that BicC may mediate many protein-protein interactions (lanes 9 and 10).

The ability of Sam68, GRP33, GLD-1, and Qk1 to self-associate and associate with each other or unrelated KH domain proteins FMR1 and BicC was examined by cotransfection in HeLa cells. Cells were transfected with the plasmid expressing HA-Sam68 alone (Fig. 9A, lanes 1 to 3) or cotransfected with plasmids expressing HA-Sam68 and myc-Sam68 (lanes 4 to 6), HA-Sam68 and myc-FMR1 (lanes 7 to 9), HA-Sam68 and myc-GLD-1 (lanes 10 to 12), HA-Sam68 and myc-GRP33 (lanes 13 to 15), and HA-Sam68 and myc-Qk1 (lanes 16 to 18). The cells were lysed, immunoprecipitated with control or anti-myc antibodies, and immunoblotted with anti-HA antibodies. HA-Sam68 was observed only in myc-Sam68 and myc-GRP33 immunoprecipitates (lanes 6 and 15, Sam68 panel). Similar experiments were performed with all the myc constructs described above with HA-GLD-1, HA-GRP33, and HA-Qk1. HA-GLD-1 was observed in myc-GLD-1 and myc-Qk1 immunoprecipitates (lanes 12 and 18, GLD-1 panel). This demonstrated that GLD-1 self-associated and associated with Qk1. HA-Qk1 was observed in myc-GLD-1 and myc-Qk1 immunoprecipitates (lanes 12 and 18, Qk1 panel). These findings demonstrated that Qk1 self-associated. HA-GRP33 was observed in myc-GRP33 immunoprecipitates, indicating that GRP33 self-associated (lane 15, GRP33 panel). We suspect that the inability of myc-Sam68 to immunoprecipitate HA-GRP33 is due to the interference of the epitope tags.

The ability of FMR1 to associate with Sam68 family members was tested. myc-FMR1 was cotransfected with HA-Sam68, HA-FMR1, HA-GLD-1, HA-GRP33, and HA-Qk1. myc-FMR1 was observed only in HA-FMR1 immunoprecipitates, demonstrating that FMR1 interacted only with itself (Fig. 9B, lane 9). We next tested whether Sam68 family members could associate with BicC. BicC was transfected alone or cotransfected with myc-Sam68, myc-FMR1, myc-GLD-1, myc-GRP33, and myc-Qk1. BicC was observed in myc immunoprecipitates of Sam68, GLD-1, GRP33, and Qk1 but not FMR1 (Fig. 9A, BicC panel). This interaction demonstrates that KH domain proteins from different classes can interact. In addition, Sam68:I→N and Sam68:G→D also associated with BicC (data not shown). In summary, GRP33, GLD-1, and Qk1 self-associated (Fig. 9C). The closest family members, GRP33 and

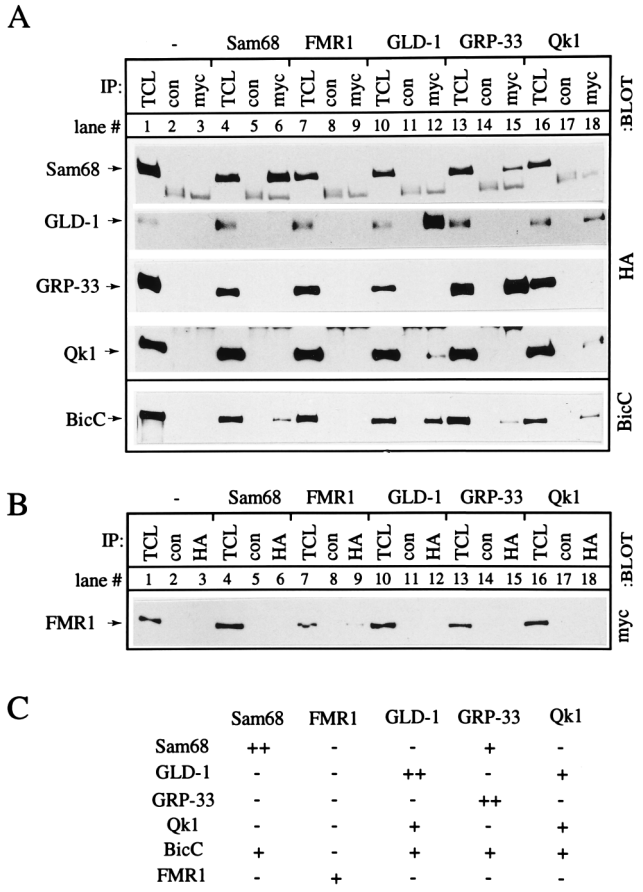

C

	Sam68	FMR1	GLD-1	GRP-33	Qk1
Sam68	++	-	-	+	-
GLD-1	-	-	++	-	+
GRP-33	-	-	-	++	-
Qk1	-	-	+	-	+
BicC	+	-	+	+	+
FMR1	-	+	-	-	-

FIG. 9. Self-association of GRP33, GLD-1, and Qk1: association with BicC but not FMR1. (A) The HA epitope-tagged Sam68, GLD-1, GRP33, or Qk1 or untagged BicC was transfected alone or cotransfected with myc-tagged Sam68, FMR1, GLD-1, GRP33, or Qk1. The cells were lysed, and an aliquot was kept for the total cell lysate (TCL). The remaining cell lysate was divided equally into two and immunoprecipitated (IP) with control (con) or anti-myc antibodies (myc). For GLD-1, the antibodies were covalently coupled to protein A-Sepharose. The bound proteins were separated by SDS-PAGE, transferred, and immunoblotted with anti-HA or anti-BicC antibodies. The position of the HA proteins or BicC is shown on the left. The other bands in the control and anti-myc lanes represent the antibody heavy chains. (B) myc-FMR1 was transfected alone or with HA-tagged Sam68, FMR1, GLD-1, GRP33, or Qk1. Cell lysates were divided equally into two and immunoprecipitated (IP) with control or anti-HA antibodies. The bound proteins were separated by SDS-PAGE and immunoblotted with anti-myc antibodies. The position of myc-FMR1 is shown on the left. (C) The data from panels A and B are summarized: ++, +, and − denote strong, moderate, and no association, respectively.

Sam68, interacted with each other, and the same was true for GLD-1 and Qk1. Sam68, GLD-1, GRP33, and Qk1 interacted with BicC but not with FMR1 when transfected in mammalian cells.

DISCUSSION

We have shown that Sam68 coimmunoprecipitated with itself in mammalian fibroblast cells by using truncated versions of Sam68. Sam68 also self-associated in yeast when expressed with the two-hybrid system. A single Sam68 complex of ~200 kDa was observed after in situ chemical cross-linking experiments in mammalian cells, demonstrating a degree of interaction specificity between the cross-linked Sam68 molecules. By using three different epitope-tagged Sam68 constructs, we demonstrated that the ~200-kDa complex was most likely a Sam68 homotrimer. As Sam68 associates with several SH3- and SH2-domain-containing signaling molecules (14, 22, 29, 37, 41, 43), it was surprising to observe a single complex after cross-linking. We speculate that Sam68 molecules are in closer molecular proximity with each other than in other complexes, and as a result, cross-linking studies reveal only one Sam68 complex.

The KH domain of Sam68 is embedded in a larger conserved protein motif of ~170 amino acids initially observed by Jones and Schedl (19). This protein motif spans amino acids 95 to 279 in Sam68, and the KH domain spans amino acids 157 to 256. The minimal region sufficient for self-association was from residues 103 to 269, located within the larger protein motif. Although a role for this conserved motif is unknown, in Sam68 it is necessary and sufficient for RNA-dependent self-association. It will be necessary to determine whether this region fulfills a similar function in the other Sam68 family members.

The KH domain was essential for Sam68 self-association. More specifically, the KH domain loops 1 and 4, unique to this family of single-KH-domain proteins, were required for self-association. The physiological importance of the conserved residues in these loops is underscored by three missense mutations identified in GLD-1 loops 1 and 4 that impair germ line differentiation (19). Replacement of the GLD-1 glycine 248 or 250 with arginine in loop 4 results in both loss-of-function (defective oocyte differentiation) and gain-of-function (inappropriate male sex determination in the hermaphrodite germ line) phenotypes (19). The GLD-1 proline 217-to-leucine mutation in loop 1 reverts the gain-of-function sex determination phenotype of the glycine 248-to-arginine mutation and displays the loss-of-function defective oogenesis phenotype. Based on the biochemical studies reported here, we propose that an inability of GLD-1 to self-associate may explain the loss of function caused by these mutations.

The presence of multiple KH domains in most proteins suggests that more than one KH domain is required to form specific and stable RNA interactions (16). Indeed, it has been demonstrated for hnRNP K and FMR1 that their multiple RNA binding domains are all required to optimally associate with RNA (32). The ability of the Sam68 complex to bind homopolymeric RNA demonstrates that single-KH-domain proteins can bind RNA as multimers. However, this does not exclude the possibility that KH domains interact with RNA as monomers. The multimers might have a higher affinity for RNA than the monomer and might have more than one RNA binding site. On the other hand, multimers might have different RNA binding specificities than the monomers. Multimers might interact with each other on neighboring sites on RNA, forming interactions with RNA that resemble beads on a string as seen for hnRNP particles (5).

The formation of Sam68 complexes requires cellular RNA because RNase treatment prior to mixing abolished Sam68 self-association. However, once Sam68 complexes were formed, RNase treatment had only a mild effect on Sam68 complex formation. We interpret these data as suggesting that RNA might be required for the initial steps of complex formation and that once the complex is formed, RNA is not required to maintain the complex. Alternatively, RNA could be required at all times to form and stabilize the complex. The Sam68 complex would be resistant to RNase treatment because it protects a fragment of RNA required for its association and stability. The KH domain and approximately 100 residues C-terminal were required for homopolymeric RNA binding in the presence of heparin. Sam68 glycine 178 (GLD-1 glycine 227) and isoleucine 184 (FMR1 isoleucine 304) were essential for RNA binding activity. These results are consistent

with the essential role of FMR1 isoleucine 304 in RNA binding (32) and with the data predicting that GLD-1 glycine 227 forms part of the RNA binding surface (25). Our data demonstrate that cellular RNA is required for the self-association of Sam68: G→D and Sam68:I→N with Sam68, but unlike Sam68, the RNA associated with these constructs appeared to be hypersensitive to RNases. As it is known that replacement of the isoleucine with asparagine alters the structure of the vigilin KH domain (25), we speculate that the Sam68:G→D and Sam68: I→N proteins weakly associate with RNA and are unable to form stable protein-RNA complexes. These complexes would be destabilized by temperature and RNases and stabilized with RNase inhibitors. In contrast, Sam68:E→G, the conserved glutamic acid residue identified in the *quaking* mouse (9), had no effect on homopolymeric RNA binding activity or the ability of Sam68 to self-associate. Therefore, this glutamic acid residue must be involved in a separate unidentified function. It is interesting that the mouse Qk1 was able to associate with cellular RNA but not with homopolymeric RNA. In agreement with these results, it has been observed that the *Xenopus* Qk1 can associate with *Xenopus* cellular RNA (47).

The tyrosine phosphorylation of Sam68 can be observed when overexpressed with a Src-family tyrosine kinase and/or in cells arrested in mitosis with nocodazole (14, 29, 37, 43, 45). To date, no cell surface receptor has been shown to physiologically induce the tyrosine phosphorylation of Sam68. We demonstrated previously that the coexpression of $p59^{fyn}$ with Sam68 results in Sam68 tyrosine phosphorylation (29) and that the phosphorylation of Sam68 abrogated its homopolymeric RNA binding activity (42). This was a direct effect of phosphorylation because phosphatase treatment restored RNA binding activity (42). We hypothesized two models by which RNA binding activity was inhibited by phosphorylation. The first model proposed was that Sam68 bound RNA as an oligomer and phosphorylation interfered with the oligomerization. The second model proposed was that the C-terminal tyrosine-rich region of Sam68 sterically inhibited the KH domain from accessing RNA. Since oligomerization of Sam68 was abrogated with $p59^{fyn}$, this suggested that tyrosine phosphorylation negatively regulates complex formation. Because Sam68 does not bind RNA when phosphorylated and RNA is required for self-association, oligomerization may be inhibited because the phosphorylated Sam68 is unable to bind RNA, or alternatively, RNA binding might be affected because the phosphorylated Sam68 is unable to oligomerize. Our current working model for Sam68 function is that in the nonphosphorylated state Sam68 associates with RNA and with SH3 domain proteins such as Src kinases and PLCγ as a multimer. The activation of Src-family kinases phosphorylates Sam68 and disassembles the Sam68 complex. As a result, the RNA binding activity of Sam68 would be inhibited. The tyrosine-phosphorylated monomeric form of Sam68 would now be available to associate with Grb2 via its SH2 domain, and the Src kinases and PLCγ would be available to associate with their SH3 and SH2 domains. This model suggests that the monomeric form of Sam68 is mainly involved in signaling and that the multimer is involved in RNA binding and some signaling functions. These distinct functions of Sam68 would then be regulated by tyrosine phosphorylation. Consistent with this model of Sam68 function is the discovery of a splice variant of Sam68 that contains all the signaling motifs but not the KH domain (3). This splice variant would be able to fulfill only the Sam68 signaling functions. It has been shown that this variant does not bind RNA (3), and based on the data presented here, we expect that this splice variant would be unable to self-associate.

The ability of GRP33, GLD-1, and Qk1 to oligomerize and form specific complexes after chemical cross-linking demonstrates that oligomerization is a general feature of this subfamily of KH domain proteins. Our studies demonstrate that these family members are also RNA-binding molecules. However, the regulation by tyrosine phosphorylation may not be a common property of all members, and it remains to be determined whether GRP33, GLD-1, and Qk1 are phosphoproteins. It is intriguing that GRP33 and Sam68 as well as GLD-1 and Qk1 associated with one another, implying that heteromultimers might be forming as seen for FMR and FXR proteins (46). However, we suspect that the formation of these complexes with other family members in their respective species is unlikely because of the chemical cross-linking experiments. These experiments demonstrated that a single complex for each member was formed with the exception of GLD-1 and most likely represented homomultimers. The association of Sam68 family members with BicC, a protein with five KH domains (23), demonstrates that the Sam68 family members can associate with other KH domain proteins.

In conclusion, we demonstrate that Sam68 self-associated in the presence of cellular RNA and that KH domain loops 1 and 4 were required for self-association. Sam68 formed multimers in vivo that bound homopolymeric RNA and SH3 domains in vitro. Other family members, including the *A. salina* GRP33, *C. elegans* GLD-1, and the mouse Qk1, also oligomerized. These observations indicate that the single KH domain found in the Sam68 family can mediate both protein-RNA and protein-protein interactions.

ACKNOWLEDGMENTS

We thank John Hiscott, Antonis Koromilas, Louise Larose, Tim Schedl, Andrey Shaw, and André Veillette for valuable comments and for critically reading the manuscript. The homopolymeric RNA binding analysis was initiated in Andrey Shaw's laboratory. We warmly acknowledge this and thank him for his constant encouragement. We are grateful to Stephen Elledge for the use of the yeast two-hybrid components. We thank Stephen Warren for the human FMR1 cDNA, André Veillette for anti-fyn antibodies, and Mary Sutherland for screening the mouse cDNA library. We thank the members of the Terry Fox Group in Molecular Oncology for stimulating discussions.

B.B.D. is supported with funds from a Canderel fellowship. C.H. is supported by a Challenge 1996 summer award. P.L. is supported by grants from the National Cancer Institute of Canada (NCIC) with funds from the Canadian Cancer Society and is a Research Scientist of the NCIC. This work was supported by grants from the Medical Research Council of Canada and from an establishment grant from the Fonds de la Recherche en Santé du Québec to S.R. S.R. is a Scholar of the Medical Research Council of Canada.

REFERENCES

1. **Arning, S., P. Gruter, G. Bilbe, and A. Kramer.** 1996. Mammalian splicing factor SF1 is encoded by variant cDNAs and binds to RNA. RNA **2:**794–810.
2. **Ashley, C. T., K. D. Wilkinson, D. Reines, and S. T. Warren.** 1993. FMR1 protein: conserved RNP family domains and selective RNA binding. Science **262:**563–566.
3. **Barlat, I., F. Maurier, M. Duchesne, E. Guitard, B. Tocque, and F. Schweighoffer.** 1997. A role for Sam68 in cell cycle progression antagonized by a spliced variant within the KH domain. J. Biol. Chem. **272:**3129–3132.
4. **Bunnell, S. C., P. A. Henry, R. Kolluri, T. Kirchhausen, R. J. Rickles, and L. J. Berg.** 1996. Identification of Itk/Tsk Src homology 3 domain ligands. J. Biol. Chem. **271:**25646–25656.
5. **Burd, C. G., and G. Dreyfuss.** 1994. Conserved structures and diversity of functions of RNA-binding proteins. Science **265:**615–621.
6. **Cruz-Alvarez, M., and A. Pellicer.** 1987. Cloning of a full-length complementary cDNA for a *Artemia salina* glycine-rich protein. J. Biol. Chem. **262:**13377–13380.
7. **DeBoulle, K., A. J. M. H. Verkerk, E. Reyniers, L. Vits, J. Hendrickx, B. V. Roy, F. V. D. Bos, E. DeGraaff, B. A. Oostra, and P. J. Willems.** 1993. A point mutation in the FMR-1 gene associated with fragile X mental retardation. Nat. Genet. **3:**31–35.
8. **Durfee, T., K. Becherer, P. L. Chen, S. H. Yeh, Y. Yang, A. E. Kilburn, W. H.**

Lee, and S. J. Elledge. 1993. The retinoblastoma protein associates with the protein phosphatase type 1 catalytic subunit. Genes Dev. **7:**555–569.
9. **Ebersole, T. A., Q. Chen, M. J. Justice, and K. Artzt.** 1996. The *quaking* gene unites signal transduction and RNA binding in the developing nervous system. Nat. Genet. **12:**260–265.
10. **Evan, G. I., and J. M. Bishop.** 1985. Isolation of monoclonal antibodies specific for the human c-myc protooncogene product. Mol. Cell. Biol. **4:** 2843–2850.
11. **Fields, S., and O. Song.** 1989. A novel genetic system to detect protein-protein interactions. Nature **340:**245–246.
12. **Francis, R., M. K. Barton, J. Kimbel, and T. Schedl.** 1995. Control of oogenesis, germline proliferation and sex determination by the *C. elegans* gene *gld-1*. Genetics **139:**579–606.
13. **Francis, R., E. Maine, and T. Schedl.** 1995. GLD-1, a cell-type specific tumor suppressor gene in *C. elegans*. Genetics **139:**607–630.
14. **Fumagalli, S., N. F. Totty, J. J. Hsuan, and S. A. Courtneidge.** 1994. A target for Src in mitosis. Nature **368:**867–871.
15. **Fusaki, N., A. Iwamatsu, M. Iwahima, and J. Fujisawa.** 1997. Interaction between Sam68 and Src family tyrosine kinases, fyn and lck, in T cell receptor signaling. J. Biol. Chem. **272:**6214–6219.
16. **Gibson, T. J., J. D. Thompson, and J. Heringa.** 1993. The KH domain occurs in a diverse set of RNA-binding proteins that include the antiterminator NusA and is probably involved in binding to nucleic acid. FEBS Lett. **324:** 361–366.
17. **Hardy, R. J., C. L. Loushin, V. L. Friedrich, Jr., Q. Chen, T. A. Ebersole, R. A. Lazzarini, and K. Artzt.** 1996. Neural cell type-specific expression of QKI proteins is altered in the *quaking* viable mutant mice. J. Neurosci. **16:**7941–7949.
18. **Jones, A. R., R. Francis, and T. Schedl.** 1996. GLD-1, a cytoplasmic protein essential for oocyte differentiation, shows stage- and sex-specific expression during *Caenorhabditis elegans* germline development. Dev. Biol. **180:**165–183.
19. **Jones, A. R., and T. Schedl.** 1995. Mutations in GLD-1, a female germ cell-specific tumor suppressor gene in *C. elegans*, affect a conserved domain also found in Sam68. Genes Dev. **9:**1491–1504.
20. **Lawe, D. C., C. Hahn, and A. J. Wong.** 1997. The Nck SH2/SH3 adaptor protein is present in the nucleus with the nuclear protein Sam68. Oncogene **14:**223–231.
21. **Lock, P., S. Fumagalli, P. Polakis, F. McCormick, and S. A. Courtneidge.** 1996. The human p62 cDNA encodes Sam68 and not the ras-GAP-associated p62 protein. Cell **84:**23–24.
22. **Maa, M.-C., T.-H. Leu, B. J. Trandel, J.-H. Chang, and S. J. Parsons.** 1994. A protein that is related to GTPase activating protein-associated p62 complexes with phospholipase Cγ. Mol. Cell. Biol. **14:**5466–5473.
23. **Mahone, M., E. E. Saffman, and P. F. Lasko.** 1995. Localised Bicaudal-C RNA encodes a protein containing a KH domain, the RNA-binding motif for FMR1. EMBO J. **14:**2043–2055.
24. **McBride, A. E., A. Schlegel, and K. Kirkegaard.** 1996. Human protein Sam68 relocalization and interaction with poliovirus RNA polymerase in infected cells. Proc. Natl. Acad. Sci. USA **93:**2296–2301.
25. **Musco, G., G. Stier, C. Joseph, M. A. Morelli, and A. Pastore.** 1996. Three-dimensional structure and stability of the KH domain: molecular insights into the fragile X syndrome. Cell **85:**237–245.
26. **Nussbaum, R. L., and D. H. Ledbetter.** 1995. The fragile X syndrome, p. 795–810. *In* C. R. Scriver, A. Beaudet, W. S. Sly, and D. Valles (ed.), Metabolic basis of inherited disease. McGraw-Hill, New York, N.Y.
27. **Pawson, T.** 1995. Protein modules and signalling networks. Nature **373:**573–580.
28. **Pieretti, M., F. Zhang, Y.-H. Fu, S. T. Warren, B. A. Oostra, C. T. Caskey, and D. L. Nelson.** 1991. Absence of expression of the FMR-1 gene in fragile X syndrome. Cell **66:**817–822.
29. **Richard, S., D. Yu, K. J. Blumer, D. Hausladen, M. W. Olszowy, P. A. Connelly, and A. S. Shaw.** 1995. Association of p62, a multifunctional SH2- and SH3-domain-binding protein, with src family tyrosine kinases, Grb2, and phospholipase Cγ-1. Mol. Cell. Biol. **15:**186–197.
30. **Richard, S., and H. H. Zingg.** 1991. Identification of a retinoic acid response element in the human oxytocin promoter. J. Biol. Chem. **266:**21428–21433.
31. **Sidman, R. L., M. M. Dickie, and S. H. Appel.** 1964. Mutant mice (quaking and jimpy) with deficient myelination in the central nervous system. Science **144:**309–311.
32. **Siomi, H., M. Choi, M. C. Siomi, R. L. Nussbaum, and G. Dreyfuss.** 1994. Essential role for KH domain in RNA binding: impaired RNA binding by a mutation in the KH domain of FMR1 that causes fragile X syndrome. Cell **77:**33–39.
33. **Siomi, H., M. J. Matunis, W. M. Michael, and G. Dreyfuss.** 1993. The pre-mRNA binding K protein contains a novel evolutionarily conserved motif. Nucleic Acids Res. **21:**1193–1198.
34. **Siomi, M. C., Y. Zhang, H. Siomi, and G. Dreyfuss.** 1996. Specific sequences in the fragile X syndrome protein FMR1 and the FXR proteins mediate their binding to 60S ribosomal subunits and the interaction among them. Mol. Cell. Biol. **16:**3825–3832.
35. **Taggart, A. K. P., and B. F. Pugh.** 1996. Dimerization of TFIID when not bound to DNA. Science **272:**1331–1333.
36. **Taylor, S. J., M. Anafi, T. Pawson, and D. Shalloway.** 1995. Functional interaction between c-src and its mitotic target, Sam68. J. Biol. Chem. **270:** 10120–10124.
37. **Taylor, S. J., and D. Shalloway.** 1994. An RNA-binding protein associated with src through its SH2 and SH3 domains in mitosis. Nature **368:**867–871.
38. **Toda, T., A. Iida, T. Miwa, Y. Nakamura, and T. Imai.** 1994. Isolation and characterization of a novel gene encoding nuclear protein at a locus (D11S636) tightly linked to multiple endocrine neoplasia type 1 (MEN1). Hum. Mol. Genet. **3:**465–470.
39. **Trub, T., J. D. Frantz, M. Miyazaki, H. Band, and S. E. Shoelson.** 1997. The role of a lymphoid-restricted, Grb2-like SH3-SH2-SH3 protein in T cell receptor signaling. J. Biol. Chem. **272:**894–902.
40. **Verkerk, A. J. M. H., M. Pieretti, J. S. Sutcliffe, Y.-H. Fu, D. P. Kuhl, A. Pizzuti, O. Reiner, S. Richards, M. F. Victoria, F. Zhang, B. E. Eussen, G. J. B. van Ommen, L. A. J. Blonden, G. J. Riggins, J. L. Chastain, C. B. Kunst, H. Galjaard, C. T. Caskey, D. L. Nelson, B. A. Oostra, and S. T. Warren.** 1991. Identification of a gene (FMR1) containing a CGG repeat coincident with a breakpoint cluster region exhibiting length variation in fragile X syndrome. Cell **65:**905–914.
41. **Vogel, L. B., and D. J. Fujita.** 1995. p70 phosphorylation and binding to p56lck is an early event in interleukin-2 induced onset of cell cycle progression in T-lymphocytes. J. Biol. Chem. **270:**2506–2511.
42. **Wang, L. L., S. Richard, and A. S. Shaw.** 1995. p62 association with RNA is regulated by tyrosine phosphorylation. J. Biol. Chem. **270:**2010–2013.
43. **Weng, A., S. M. Thomas, R. J. Rickles, J. A. Taylor, A. W. Brauer, C. Seidel-Dugan, W. M. Michael, G. Dreyfuss, and J. S. Brugge.** 1994. Identification of Src, Fyn, and Lyn SH3-binding proteins: implications for a function of SH3 domains. Mol. Cell. Biol. **14:**4509–4521.
44. **Wilson, R., R. Ainscough, K. Anderson, C. Baynes, M. Berks, J. Bonfield, J. Burton, M. Connell, T. Copsey, J. Cooper, et al.** 1994. 2.2 Mb of contiguous nucleotide sequence from chromosome III of *C. elegans*. Nature **368:** 32–38.
45. **Wong, G., O. Muller, R. Clark, L. Conroy, M. F. Moran, P. Polakis, and F. McCormick.** 1992. Molecular cloning and nucleic acid binding properties of the GAP-associated tyrosine phosphoprotein p62. Cell **69:**551–558.
46. **Zhang, Y., J. P. O'Connor, M. C. Siomi, S. Srinivasan, A. Dutra, R. L. Nussbaum, and G. Dreyfuss.** 1995. The fragile X mental retardation syndrome protein interacts with novel homologs FXR1 and FXR2. EMBO J. **14:**5358–5366.
47. **Zorn, A. M., M. Grow, K. D. Patterson, T. A. Ebersole, Q. Chen, K. Artzt, and P. A. Krieg.** 1997. Remarkable sequence conservation of transcripts encoding amphibian and mammalian homologues of *quaking*, a KH domain RNA-binding protein. Gene **188:**199–206.